NOAA Technical Memorandum NWS ER-81

Relation of Wind Field and Buoyancy to Rainfall Inferred from Radar

Hugh M. Stone
National Weather Service Eastern Region
Bohemia, New York

Scientific Services Division
Eastern Region Headquarters
April 1989

U.S. DEPARTMENT OF COMMERCE / National Oceanic and Atmospheric Administration / National Weather Service

NOAA TECHNICAL MEMORANDUM NWS ER-81

RELATION OF WIND FIELD AND BUOYANCY TO RAINFALL INFERRED FROM RADAR

Hugh M. Stone
National Weather Service Eastern Region
Bohemia, New York

Scientific Services Division
Eastern Region Headquarters
April 1989

RELATION OF WIND FIELD AND BUOYANCY TO RAINFALL INFERRED FROM RADAR

Hugh M. Stone

Eastern Region Headquarters
National Weather Service, NOAA
Bohemia, New York

I. INTRODUCTION

Forecasting the potential for heavy rain, which may cause flash flooding is one of the most important activities of the National Weather Service. The problem is difficult because heavy rain events are usually the result of small scale convective storms and frequently occur with a synoptic map pattern that appears very benign.

Maddox et.al. (1979) compiled a 5-year climatology of flash flood events from 1973 to 1977 and classified the heavy rain events into three types: synoptic, frontal, and mesohigh. Synoptic events characteristically involve a major trough at 500 mb moving slowly east or northeastward and an associated surface system with convective storms continuously developing and moving over the same area. This type of event occurs mostly frequently in spring and fall when favorable dynamic and thermodynamic conditions prevail. Frontal type flash flood events involve a stationary or slow moving frontal boundary usually oriented east-west which serves to trigger and focus heavy rain on the cool side of the front as warm unstable air flows over the front. Mesohigh events are similar but much smaller scale and associated with a nearly stationary thunderstorm outflow boundary generated by prior convection. Heavy rain occurs on the cool side of the boundary.

Various features are common to all the flash flood types: heavy rains are from convective storms, large surface dewpoints are present, large moisture content prevails through a deep tropospheric layer, and vertical wind shear is weak to moderate through the cloud depth.

To get a heavy rain accumulation from convective storms it is essential that the storms be stationary or slow moving or several storms must pass over the same area. Fast moving cells may have high rainfall rates but their resultant rainfall is usually not excessive at any point because the rain does not last for long. The motion of a storm complex may be considered as the sum of two vectors: the velocity vector of the individual cell motion plus the propagation velocity due to new cells discretely forming along the periphery of the storm complex (Chappell, 1986). The vector of mean cell motion lies along or to either side of the vector mean wind of the cloud layer. Propagation may occur anywhere on the cell periphery. A diagram showing the effect of propagation

on storm motion is shown in Fig. 1. It is evident that propagation may either accelerate or decelerate storm motion or deflect it to either side of the mean cell motion. If the propagation vector is directly opposite the mean cell velocity vector, the resultant may be zero storm motion (Fig.1), the condition that leads to excessive rainfall and flash floods.

Backward propagating mesoscale convective systems (MCS) usually produce heavier rainfall and more flash floods than forward propagating systems. Shi and Scofield (1987) have identified several characteristics favorable for backward propagation of an MCS: wind maximum at 850 mb with warm unstable air being advected into an area or an area of instability being lifted by 500 mb positive vorticity advection (PVA), convective outflow or frontal boundary present, east-west orientation of thickness pattern, and weak mid to upper level flow.

The development of quasi-stationary MCSs appears to occur most frequently as the storm complex moves past the most unstable air across the band of maximum low level winds, and in the region of strongest moisture convergence (Chappell, 1986). When this situation is achieved the trend is for thunderstorms on the leading edge of the MCS to decay, while new cell generation occurs on the rear flank of the storm, forming a slow moving or stationary MCS.

Mean hodographs were constructed for the three types of flash floods provided in the data sample from Maddox (1979) and the results are shown in Fig. 2. All three hodographs show an easterly component for the surface wind and a relatively strong southerly component for the 850 mb level wind. An easterly wind at the surface causes the outflow boundary from the main storm to move primarily westward providing a triggering mechanism for new cell growth on the rear flank of the storm, while the southerly flow at 850 mb feeds a fresh supply of moist unstable air to the newly developing cells.

The numerical cloud modelling studies of Weisman and Klemp (1986) indicate that environmental wind shear has a strong influence on the type of convection that develops, supercell convection developing in high shear conditions and multicell convection in low shear conditions. The best way to examine wind shear is with the aid of a hodograph, which also allows a rough estimate of cell motion to be made. Given the same wind shear structure, a westerly surface wind moves the cells more rapidly eastward while an easterly component to the surface wind has the effect of slowing down cell motion possibly even stopping it. Since the hodograph may be a useful tool for evaluating the potential for heavy rainfall, a sample of data was collected over the midwest and eastern United States during the warm season of 1988, and various features of the wind field were correlated to rainfall inferred from VIP levels over the MDR grid.

II. METHOD

Wind profile data and stability/buoyancy data were collected from seventeen locations in the Midwest and East where raob observation sites are colocated with network radar sites (Fig.3). Radar and raob data were obtained automatically by a data collection program, which extracted operationally available data from the AFOS circuit. Raob data from both synoptic times 0000 UTC and 1200 UTC were used in the analysis. Due to various problems with the computer system only about 35 percent of the potentially available data were saved. U and V wind components were computed and linearly interpolated from the standard reporting levels to exactly one thousand foot intervals from the surface to sixteen thousand feet above ground level (AGL). Several measures of wind shear were computed from these wind profiles: the vector product shears VS5, VS10, and VS15, the speed shears SS5, SS10, and SS15 and the shear SHR used in the computation of Bulk Richardson Number; these have all been previously defined in Stone (1988b). An additional wind parameter ,NEGU5, was computed which is the sum of the negative "U" wind components from the surface to five thousand feet AGL. Five buoyancy parameters were tabulated: the energy index (EI) which is computed by integrating the positive and negative energy areas of a parcel ascending from the level with maximum wet bulb potential temperature to the 400 mb level while entraining environmental air during the ascent (Stone, 1984). EI+ and EI- are the positive and negative parts of EI. Positive and negative buoyancies B+ and B- were tabulated and these represent the buoyancies of a saturated parcel ascending with zero entrainment from the convective condensation level (CCL) to the equilibrium level (EL).

Direct rainfall data were not used, but precipitation amounts were inferred from radar using accumulated VIP levels over the MDR grid. The relation between radar VIP level and rainfall intensity is not very accurate due to varying drop size distribution in rain clouds, radar attenuation, and various other factors. Nevertheless, high VIP levels are generally associated with heavy rain and low VIP levels with lighter rain. Heavy rain events that can cause flash floods are mostly commonly caused by a stationary convective cell or the passage of several cells over the same area. A high VIP level occurring in a particular MDR box for several hours should be indicative of a heavy rain event.

The twelve hour period following each of the standard synoptic hours 0000 UTC and 1200 UTC was examined for the persistence of various VIP levels in each MDR box within 100 nautical miles of the radar site. A count was made for each MDR box of the number of hours that VIP level equals or exceeds level 3 and level 5. The maximum number of hours of level 3 or level 5 in any of the boxes surrounding the radar will be denoted M3 and M5 respectively and these values will be considered as an indirect measure of maximum rainfall in the area within a 100 nautical mile radius of the radar/raob site. If any single hour of radar data was missing, that missing VIP value was interpolated or

extrapolated from the preceding and/or following hour. If two consecutive hours were missing, then that case was rejected and not used in the statistical analysis. Interpolation of a single hour was done to avoid decreasing the sample size, since missing data over a twelve hour period is not an uncommon occurrence.

III. RESULTS

Standard correlation coefficients were computed between M3 and the various buoyancy and wind shear measures. The sample was first stratified by season and geographic area. Spring season is considered to be the months of April, May, and June, and summer season July, August, and September. Midwest and eastern areas are indicated in Fig. 3. The resulting correlation coefficients are shown in Table 1.

The best single correlation was from the EI in both seasons and both geographic areas. The buoyancy parameter B+ was not as good as EI probably due to the fact that B+ is computed using an undiluted saturated parcel while EI uses a parcel with an entrainment process and is therefore sensitive to environmental moisture. Correlation of all the wind shear parameters to M3 is rather poor. The vector product shears VS5, VS10, and VS15 yield the best results in the spring season. In the summer they are statistically significant only in the east. The parameter NEGU5, the sum of negative "U" components to five thousand feet, yielded a poor correlation that was not statistically significant.

Table 2 shows correlations to M3 for the combined data without seasonal or geographic stratification. Of the 2145 cases in the combined sample, 871 of these had VIP levels of 3 or more, all the others, 59 percent of the sample, had VIP levels of less than 3. We have previously determined that EI is well related to the observed VIP level (Stone, 1985). Since most of the sample consists of cases with M3 equal zero, it seems possible that the correlation may be unduly influenced by this portion of the sample, i.e. the parameter being correlated is discriminating between cases with M3 = 0 and cases with M3 $\geq$ 1. Therefore, all the cases with zero M3 were removed from the sample and correlations were recomputed. The results are shown in the second column of Table 2. We see that all the statistically significant correlations of column 1 are greatly reduced in column 2, with the wind shear correlations becoming insignificant, some reduced to zero. The energy index continues to be statistically significant and has better correlation than any of the other buoyancy parameters.

The poor relationship of wind shear to M3 suggested that correlations be computed for all the "U" and "V" components of the hodograph from the surface to 16 thousand feet AGL. These results are shown in Table 3 with the full sample in the left column and a reduced sample with M3 = 0 removed in the right column. All of the "U" component correlations are very poor, although the surface component U0 is statistically significant. The negative U0

correlation means that there is some tendency for easterly surface winds to be associated with large M3 but the correlation -.087 is very low. Considerably better correlations are obtained with the "V" wind components, in particular those above 5 thousand feet AGL, although they are not very good when cases with M3 = 0 are removed. The significant correlations of surface "U" component and mid-level "V" components should be expected since easterly surface flow and southerly mid level flow are characteristic of conditions associated with flash flood events (Fig. 2).

Composite mean hodographs were computed according to the value of M3, using the same data from which the previously discussed correlation coefficients were computed. The results are shown in Fig. 4 for the spring season and Fig. 5 for the summer. The western hodographs in springtime (Fig. 4.) show a tendency for easterly surface winds to be associated with large values of M3, however, this tendency is not seen in the eastern hodographs. The summer hodograph in the west (Fig. 5.) for M3 of 6 hours or more also shows easterly surface winds, but there is little evidence of this in the eastern hodographs on the right side of the figure. In all the hodographs of Fig. 4. and Fig. 5. there is a tendency for strong southerly winds at mid levels to be associated with high values of M3. Of course, all of this is consistent with the correlations in Table 3.

Similar composite hodographs were prepared for various values of M5, the number of hours of peristence of VIP level 5 or more in an MDR box. These are shown in Fig. 6. for spring and Fig. 7. for summer. The hodographs are roughly of the same form as those obtained stratifying data according to the value of M3. There is a general veering of the shear vector with height in most of them, and a weak relationship between value of M5 and surface "U" components and mid level "V" components is still evident, but the relationship is not as good as that seen when hodographs are composited according to value of M3. This apparent deterioration in the relationship may be due to the small sample of long-lived VIP level 5 events.

The mean hodographs composited according to the persistence of M3, VIP level 3, (Figs. 4 and 5) show much variability. Except for the Midwest in spring, there is no definite trend in the hodographs as hours of M3 increase. However, there are similarities among the long-lived VIP level 3 hodographs shown at bottom of both figures: there is an easterly surface wind component in all of them, although very small in the east, there is a relatively strong southerly wind component at around 5 thousand feet AGL, and strongest wind shears occur near the surface with the shear vector veering with height. These are general characteristics of the wind field associated with heavy rainfall, but the forecaster should remember that these are mean hodographs and there is considerable variation among the individual hodographs that comprise the mean.

IV. CONCLUSIONS

The results presented above are in agreement with both theoretical (Weisman and Klemp, 1986) and prior observational studies (Maddox, 1979) which indicate that excessive rainfall events are associated with a particular form of hodograph. An easterly wind at the surface with strong southerly flow around 850 mb is favorable for stationary or slow moving convective storms. The easterly surface wind causes the outflow boundary to move primarily westward allowing new cells to form on the rear flank of the main storm, while the southerly flow of moist unstable air at low levels provides the fuel to feed the growing cells. Mean hodographs constructed from mandatory level wind data, which was interpolated subjectively in both space and time for documented flash flood events (Maddox, 1979) are shown in Fig. 2 and exhibit this characteristic structure.

Our data sample does not include any noteable flash flood events, but the heavy rain (long-lived VIP level 3 and 5) cases generally have the same features as the Maddox (1979) hodographs, except our wind shear is not as strong. This may be due to the fact that our events are not as extreme and we are not interpolating in space and time to get a proximity hodograph. Figures 4 and 5 show a seasonal variation of hodograph forms in the Midwest between spring and summer. In the East only the springtime hodograph associated with VIP level 3 persisting for five or more hours (Fig. 4) has some similarity to the hodographs of Maddox, but these similarities diminish during the summer season (Fig. 5). These seasonal and geographic differences are not necessarily typical since our data is from a single year, 1988. An expanded sample covering several years may yield a somewhat different picture.

Our study uses persistence of VIP levels 3 and 5 rather than observed rainfall. The relation between VIP level and rainfall rate is not very precise, but generally high VIP levels are associated with heavy rain and lower VIP level with light rain. It seems unlikely that significantly different results would have been obtained using observed rainfall over the 12 hour period rather than the persistence of VIP values.

The rather poor relationship between rainfall inferred from VIP levels and hodograph patterns can probably be better ascribed to the variation both in time and space of the wind field. In this study the hodograph at the beginning of the twelve hour period is related to the subsequent persistence of VIP levels observed during a twelve hour period within a 100 nautical mile radius of the radar site. This is a fairly large area and the hodograph could be significantly different away from the radar site, also the time variation in the wind field could be very large over this long a time period.

There is a relationship between heavy rainfall events and the wind field, but since raobs are only available twice per day with a large distance between raob sites, it is necessary to estimate the wind profile at the time and place where convection is expected to occur. This is a difficult task but the situation will improve when a wind profiler network is established which will allow frequent temporal sampling of the vertical wind structure.

Meanwhile, the forecaster should keep in mind that the preferred wind structure for stationary convective storms is an easterly surface wind with strong southerly flow around 850 mb and decreasing wind shear above 850 mb with these conditions prevailing at the time convection is expected to begin. The synoptic and mesoscale conditions must be carefully evaluated to determine proper conditions for a backward propagating storm system which may produce excessive rainfall. In addition to the proper wind structure, several other important features are necessary: increasing instability, some type of boundary and upward vertical motion, low level moisture convergence, and plenty of moisture. Backward propagating storms usually occur when the most unstable air lies to the west of the convective system. Shi and Scofield (1987) found that the field of mean equivalent potential temperature for the layer 850 mb to 300 mb is useful for determining areas of potential backward propagation of storms. They found that storms develop in the unstable air along and to the north of the ridge line axis of this field (Fig. 8.). The field of mean wet bulb potential temperature has the same form as equivalent potential temperature and may be used for this purpose. Mean wet bulb potential temperature is available from the CONVECTA AFOS application program (Stone, 1988a). Shi and Scofield (1987) also provide a useful decision tree for examining factors that contribute to heavy rainfall.

V. REFERENCES

Chappell, C.F., 1986: Quasi-Stationary Convective Events, Mesoscale Meteorology and Forecasting, Editor P.S. Ray, Amer. Meteor. Soc., 289-310.

Maddox, R.A., C.F. Chappell, and L.R. Hoxit, 1979: Synoptic and Meso-a Scale Aspects of Flash Flood Events, Bull. Amer. Meteor. Soc., 60, 115-123.

Shi, J. and R.A. Scofield, 1987: Satellite Observed Mesoscale Convective System (MCS) Propagation Characteristics and a 3-12 Hour Heavy Precipitation Forecast Index, NOAA Technical Memorandum NESDIS 20, National Environmental Satellite, Data, and Information Services, Washington, D.C.

Stone, H.M., 1984: The Energy Index for Stability, Preprints, 10th Conf. Weather Forecasting and Analysis, Amer. Meteor. Soc., Clearwater Beach, FL, 550-554.

Stone, H.M., 1985: A Comparison Among Various Thermodynamic Parameters for the Prediction of Convective Activity, Part II, NOAA Technical Memorandum NWS ER-69, National Weather Service, Garden City, NY.

Stone, H.M., 1988a: Convection Parameters and Hodograph Program - CONVECTA & CONVECTB, NOAA Eastern Region Computer Programs and Problems, NWS ERCP No. 37 Revised, National Weather Service, Garden City, NY.

Stone, H.M., 1988b: Wind Shear as a Predictor of Severe Weather for the Eastern United States, NOAA Technical Memorandum NWS ER-75, National Weather Service, Garden City, NY.

Weisman, M.L. and J.B. Klemp, 1986: Characteristics of Isolated Convective Storms, Mesoscale Meteorology and Forecasting, Editor P.S. Ray, Amer. Meteor. Soc., 331-358.

Table 1

Correlation coefficients between various buoyancy and wind shear parameters from both 0000 UTC and 1200 UTC raobs and M3, the maximum persistence in hours of radar VIP level 3 or greater in any MDR box within 100 nautical miles of the radar/raob site. M3 may be considered as proportional to the maximum rainfall in the MDR box. "F" denotes that coefficient is statistically significant at the one percent level.

	SPRING (Apr, May, Jun)			SUMMER (Jul, Aug, Sep)	
	MIDWEST	EAST		MIDWEST	EAST
No. Cases	467	569		489	620
EI	.462 F	.458 F	EI	.509 F	.521 F
EI+	.379 F	.351 F	EI+	.513 F	.461 F
EI-	.421 F	.430 F	EI-	.442 F	.476 F
B+	.332 F	.364 F	B+	.318 F	.333 F
B-	.006	.111 F	B-	.041	.096
VS5	.184 F	.200 F	VS5	.094	.116 F
VS10	.196 F	.167 F	VS10	.101	.105 F
VS15	.197 F	.169 F	VS15	.107	.105 F
SS5	.093	.160 F	SS5	.046	.184 F
SS10	.069	.087	SS10	.006	.074
SS15	.033	.056	SS15	-.002	.049
SHR	-.012	.071	SHR	.014	.028
NEGU5	-.118	.033	NEGU5	-.022	-.078

Table 2

Correlation coefficients between various buoyancy and wind shear parameters from both 0000 UTC and 1200 UTC raobs and M3, hours of radar VIP $\geq$ 3. The first column contains the combined cases of Table 1. The second column has cases with M3 = 0 removed.

	M3 $\geq$ 0	M3 > 0
No. Cases	2145	871
EI	.493 F	.298 F
EI+	.441 F	.252 F
EI-	.447 F	.266 F
B+	.336 F	.154 F
B-	.060 F	.053 F
VS5	.135 F	.016
VS10	.126 F	-.003
VS15	.129 F	.000
SS5	.099 F	.000
SS10	.027	-.044
SS15	.000	-.071
SHR	-.006	-.010
NEGU5	-.042	-.080

Table 3

Correlation coefficients between U & V wind components from surface to 16 thousand feet AGL and M3, hours of radar VIP ≥ 3. Same data and stratification as in Table 2.

	M3 ≥ 0	M3 > 0
No. Cases	2145	871
U0	-.087 F	-.103 F
U1	-.010	-.071
U2	.019	-.058
U3	.042	-.044
U4	.047	-.035
U5	.043	-.025
U6	.034	-.022
U7	.030	-.021
U8	.026	-.021
U9	.015	-.028
U10	.003	-.039
U11	-.008	-.048
U12	-.019	-.054
U13	-.025	-.055
U14	-.029	-.058
U15	-.031	-.058
U16	-.035	-.057
V0	.132 F	-.032
V1	.190 F	-.011
V2	.249 F	.036
V3	.292 F	.078
V4	.317 F	.107 F
V5	.331 F	.130 F
V6	.333 F	.138 F
V7	.336 F	.141 F
V8	.343 F	.146 F
V9	.346 F	.146 F
V10	.347 F	.150 F
V11	.350 F	.156 F
V12	.352 F	.158 F
V13	.350 F	.160 F
V14	.352 F	.162 F
V15	.351 F	.160 F
V16	.344 F	.153 F

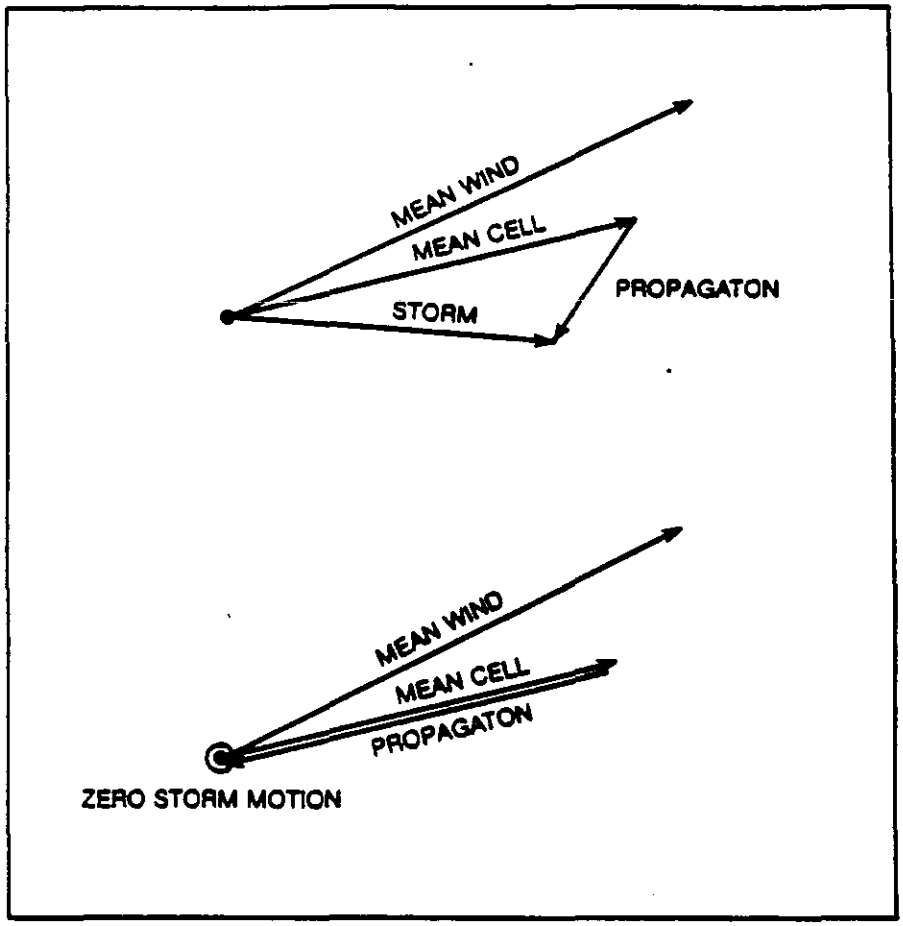

Fig. 1. Vector diagram showing the effect of propagation on storm motion (top), and the relationship between propagation and mean cell motion for developing a quasi-stationary storm complex (bottom). From Chappell (1986).

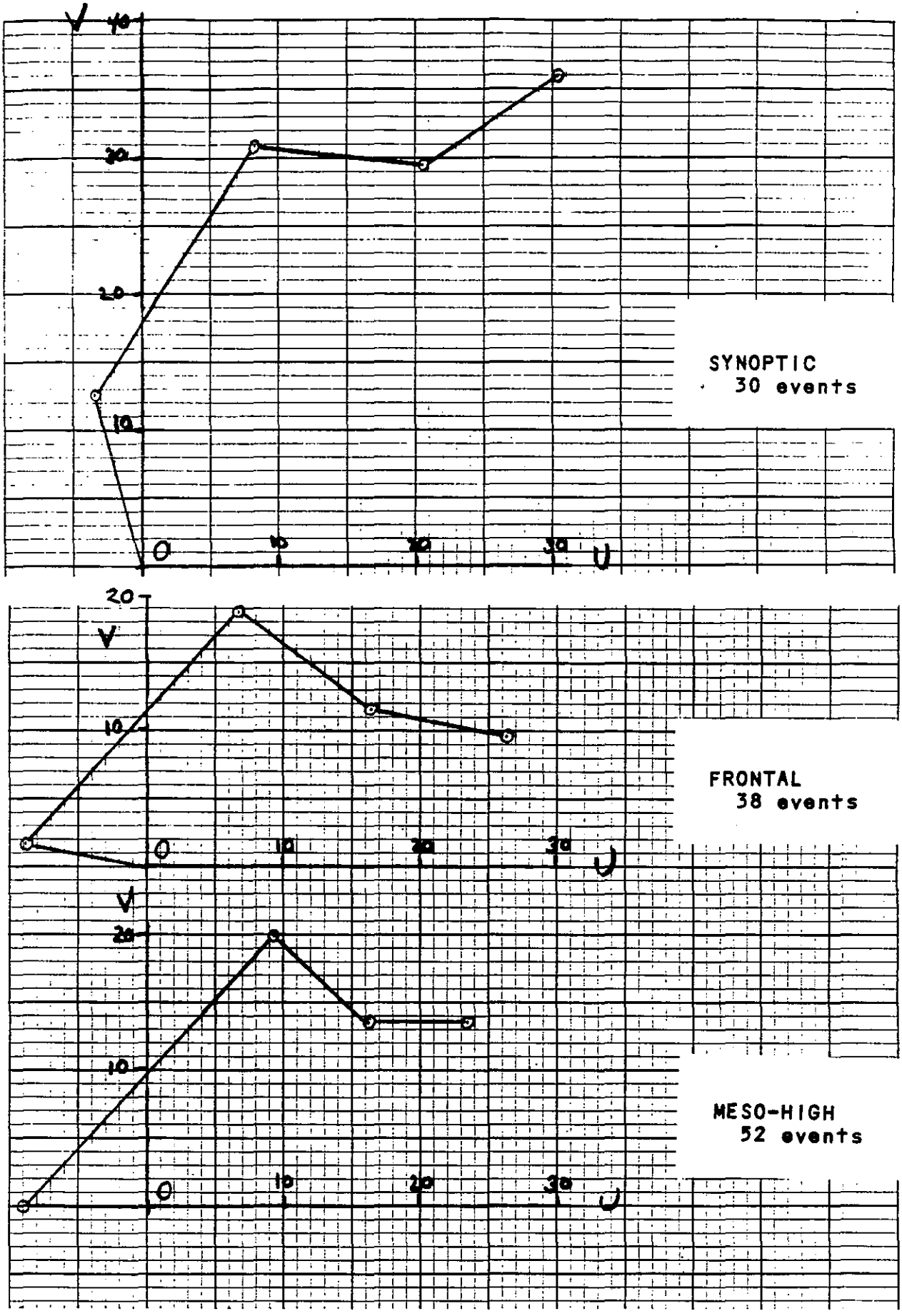

Fig. 2. Mean hodographs associated with synoptic, frontal, and meso-high type of flash floods. Units are knots. Four levels plotted: surface, 850, 700, and 500 mb. Data from Maddox (1979).

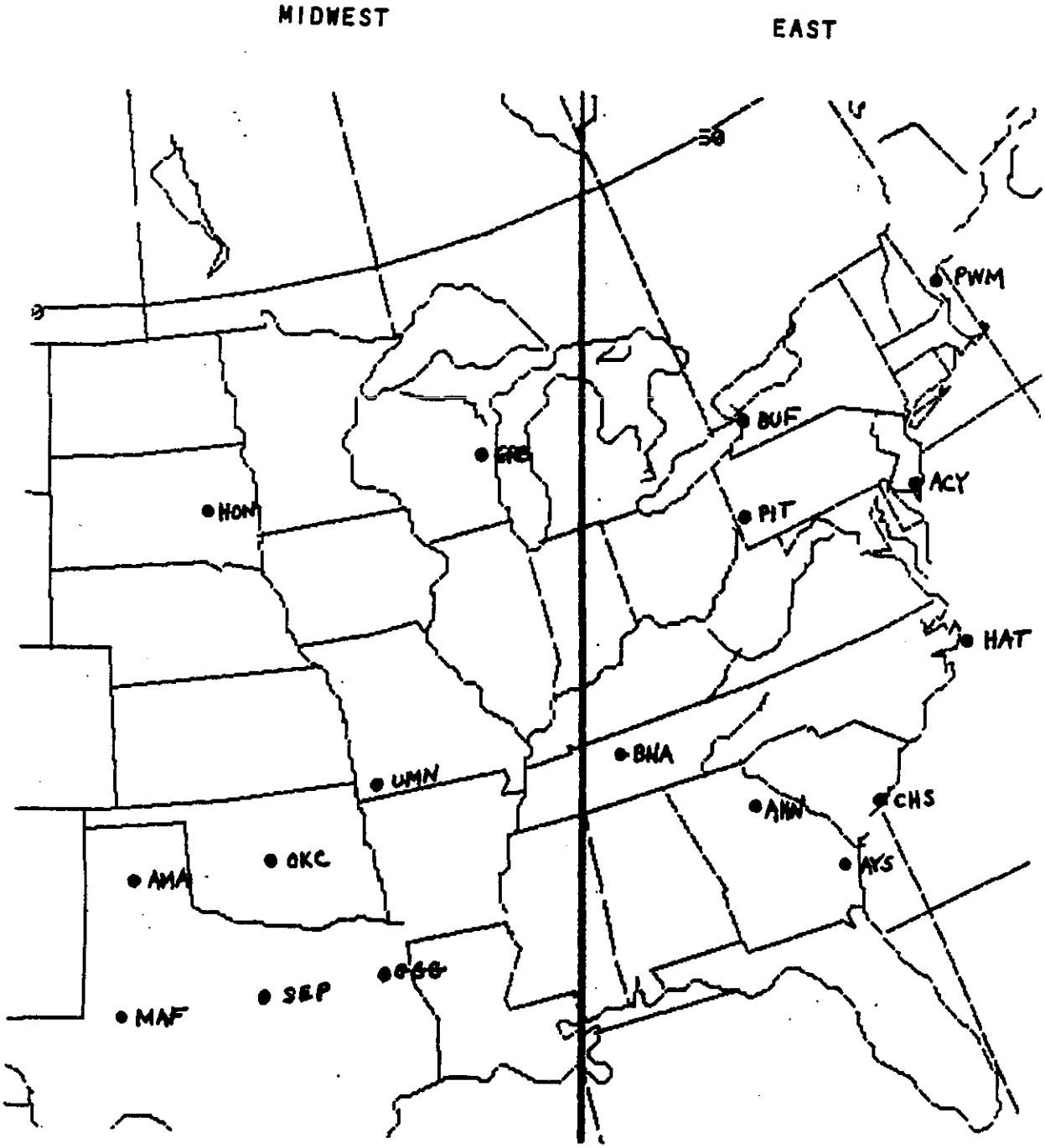

Fig. 3. Raob/radar stations used in the analysis.

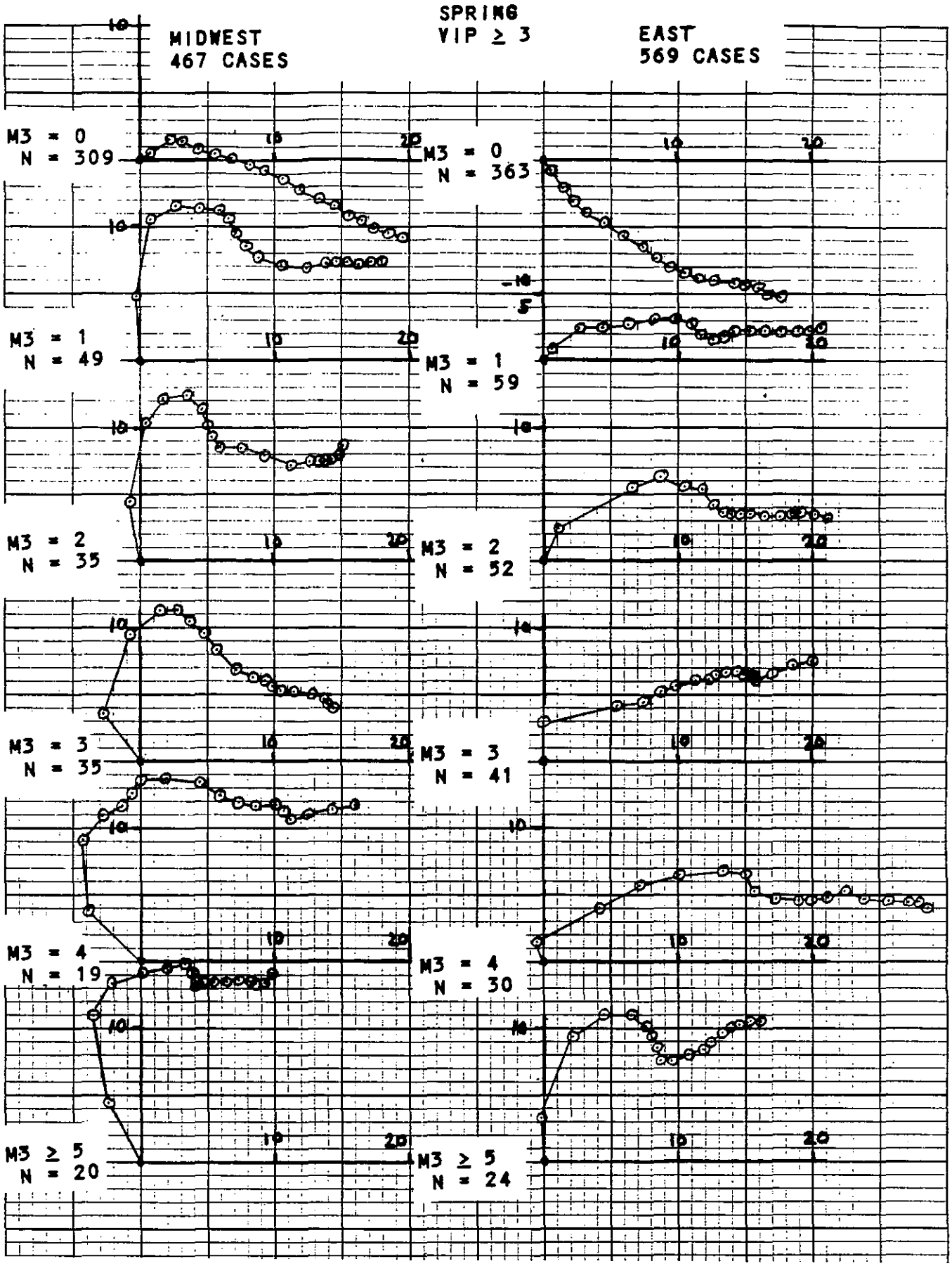

Fig. 4. Mean hodographs, surface to 16000 ft AGL, in spring season for various values of M3 (hours of radar VIP ≥ 3). Midwest region on left and east on right side. "N" denotes number of cases in each mean. Units are knots.

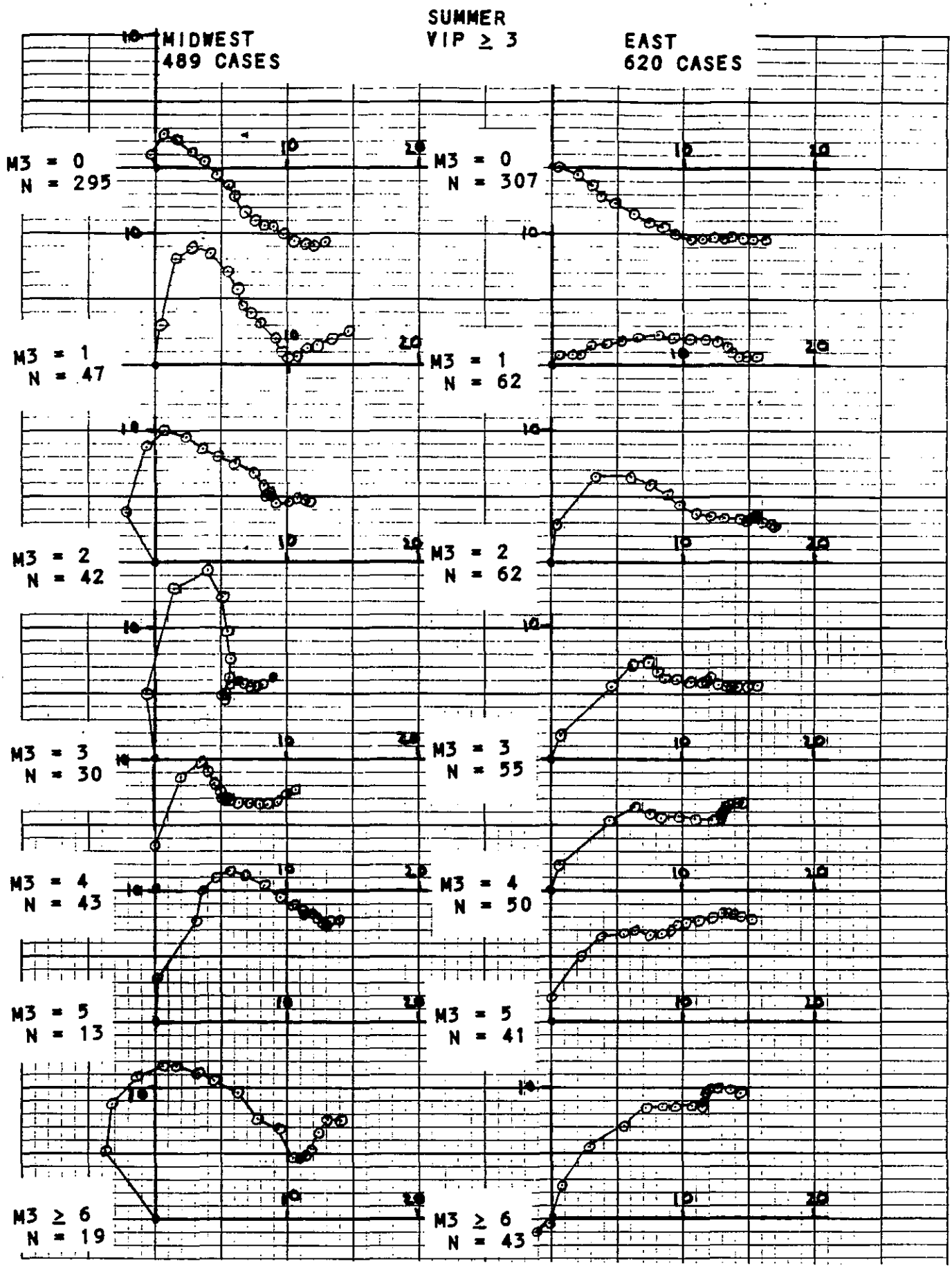

Fig. 5. Mean hodographs, surface to 16000 ft AGL, in summer season for various values of M3 (hours of radar VIP ≥ 3). Midwest region on left and east on right side. "N" denotes number of cases in each mean. Units are knots.

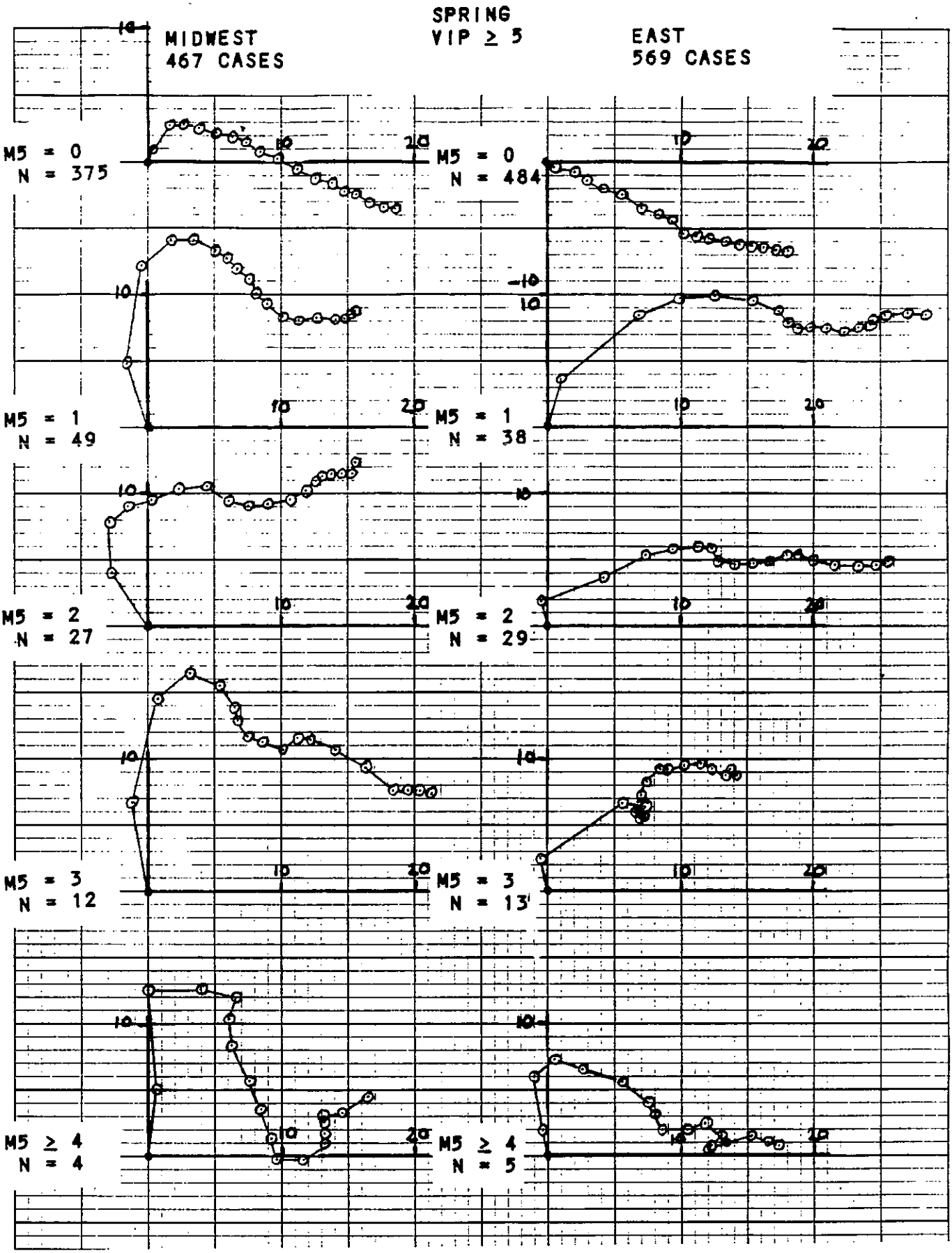

Fig. 6. Mean hodographs, surface to 16000 ft AGL, in spring season for various values of M5 (hours of radar VIP ≥ 5). Midwest region on left and east on right side. "N" denotes number of cases in each mean. Units are knots.

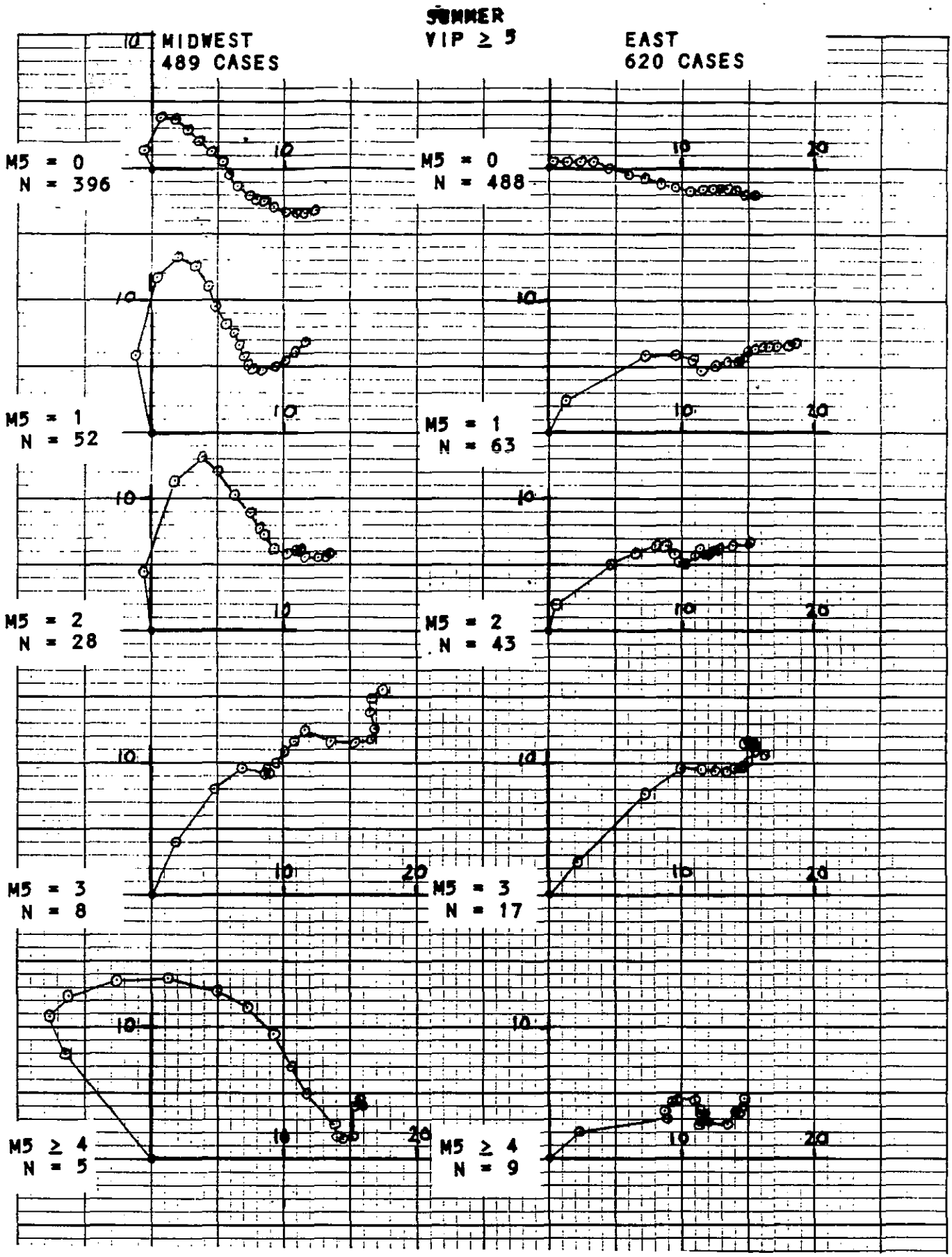

Fig. 7. Mean hodographs, surface to 16000 ft AGL, in summer season for various values of M5 (hours of radar VIP ≥ 5). Midwest region on left and east on right side. "N" denotes number of cases in each mean. Units are knots.

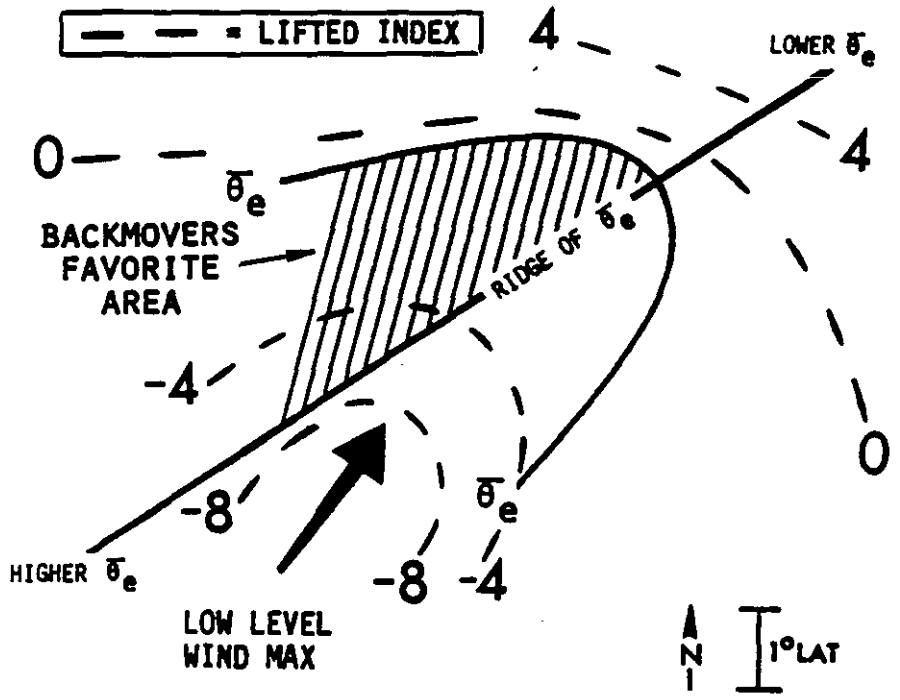

Fig. 8. Favorite area (stippled) for occurrence of backward propagating MCSs; area is located along and north of the mean equivalent potential temperature ($\bar{\theta}_e$) ridge axis. From Shi and Scofield (1987).